Degradable Vinyl Copolymer Nanoparticles/Latexes by Aqueous Nitroxide-Mediated Polymerization-Induced Self-Assembly

Maëlle Lages, Noémie Gil, Paul Galanopoulo, Julie Mougin, Catherine Lefay, Yohann Guillaneuf, Muriel Lansalot, Franck D'agosto, Julien Nicolas

Degradable Vinyl Copolymer Nanoparticles/Latexes by Aqueous Nitroxide-Mediated Polymerization-Induced Self-Assembly

*Maëlle Lages,[1] Noémie Gil,[2] Paul Galanopoulo,[3] Julie Mougin,[1] Catherine Lefay,[2] Yohann Guillaneuf,[2] Muriel Lansalot,[3] Franck D'Agosto,[3] Julien Nicolas[1,]**

[1] Université Paris-Saclay, CNRS, Institut Galien Paris-Saclay, F-91400 Orsay, France

[2] Aix Marseille Univ., CNRS, Institut de Chimie Radicalaire, UMR 7273, F-13397 Marseille, France

[3] Univ Lyon, Université Claude Bernard Lyon 1, CPE Lyon, CNRS, UMR 5128, Catalysis, Polymerization, Processes and Materials (CP2M), F-69616 Villeurbanne, France

*To whom correspondence should be addressed.

Email: julien.nicolas@universite-paris-saclay.fr

Tel.: +33 1 80 00 60 81

For Table of Contents use only

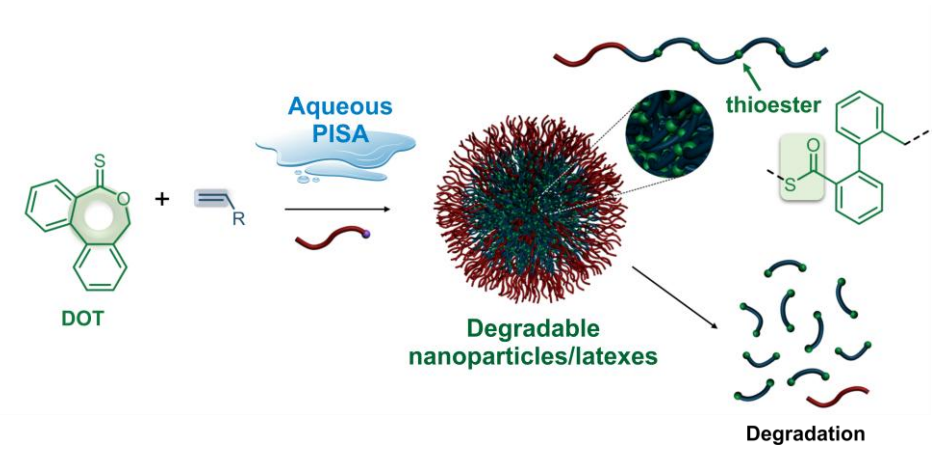

Abstract

The synthesis of degradable vinyl polymer nanoparticles/latexes in aqueous dispersed media is receiving much attention, particularly for biomedical applications and plastic pollution control, as it can circumvent the severe limitations associated with emulsification of preformed degradable polymers. Polymerisation-induced self-assembly (PISA), which enables the in-situ formation of aqueous suspensions of diblock copolymer nano-objects of high solids content, has become a very popular polymerization process due to its many advantages in terms of simplicity, robustness, scalability and versatility. However, the preparation of degradable vinyl polymer nanoparticles by direct aqueous PISA has never been reported. This severely limits the use of PISA in biomedical and environmental applications. Herein, we report the first aqueous emulsion PISA able to generate degradable vinyl polymer nanoparticles. It relies on radical ring-opening polymerization-induced self-assembly (rROPISA) of traditional vinyl monomers (*n*-butyl acrylate or styrene) with dibenzo[c,e]oxepane-5-thione (DOT), a thionolactone that features high stability in protic solvents and favourable reactivity with many vinyl monomers, and is a precursor of labile thioester groups in the main chain. Stable aqueous suspensions of thioester-containing diblock copolymer nanoparticles were obtained with both vinyl monomers. Extensive degradation of the copolymers and the nanoparticles was successfully demonstrated under aminolytic or basic conditions. Given the success of the PISA process within the polymer community, this work has the potential to greatly expand its use in many areas, from nanomedicine (providing applicability to biocompatible vinyl polymers) to degradable coatings and sustained materials.

Introduction

The design of degradable vinyl polymers is of tremendous importance for a wide range of applications such as biomaterials/nanomedicine and more environmentally friendly materials.[1] In the recent years, radical ring-opening polymerization (rROP) has offered the possibility to incorporate cleavable bonds into the backbone of vinyl polymers via a copolymerization approach (the so-called "*cleavable comonomer*" strategy).[2-4] The two main classes of monomers suitable for rROP are cyclic ketene acetals (CKAs)[5] and cyclic allylic sulfides,[6,7] and they have been used to produce various copolymers containing ester groups in the main chain.[8] However, their use is restricted due to some drawbacks: (i) the difficulty for cyclic allylic sulfides to copolymerize with vinyl monomers and the occurrence of crosslinking reactions from their remaining methylene group[6] and (ii) the low reactivity of CKA with many vinyl monomers as well as the potential ring retention during copolymerization,[2,3] resulting in low amounts of ester groups in the polymer backbone and the formation of non-degradable acetal repeat units. These monomers also exhibit limited stability upon storage and high susceptibility to hydrolysis, which severely complicate their use in polymerization in presence of protic solvents and especially in aqueous dispersed media.

This is unfortunate since polymerization-induced self-assembly (PISA)[9,10] of vinyl monomers has established as robust and versatile, surfactant-free, one-pot process to produce well-defined multiblock vinyl copolymer nanoparticles at high concentrations for a wide range of applications, spanning from Pickering emulsifiers and lubricants to nanoparticles for catalysis and biomedical applications.[10-17] Recent developments were also directed towards photo-PISA,[18,19] the tuning of the nanoparticle shape[20,21] and the development of new PISA-based processes,[22,23] among other achievements. Conferring degradability to PISA systems has been recently reported by combining PISA and rROP (termed rROPISA).[24-26] However, to prevent early degradation of CKAs, the polymerizations were performed in (non)polar aprotic solvents: (i) in heptane to generate organic dispersions of nanoparticles with CKA in the

core[24] and/or in the shell,[26] and (ii) in DMF followed by transfer to water to produce aqueous dispersions of core-degradable nanoparticles via a two-step rROPISA process.[25]

Consequently, no aqueous PISA systems leading to degradable vinyl polymer nanoparticles/latexes in one pot have been reported. As this process has become extremely popular, obtaining degradable nanoparticles by direct PISA in water remains a challenge that would greatly expand its scope of application. To the best of our knowledge, the only waterborne degradable PISA system reported so far concerns the PISA of *N*-carboxyanhydrides, which is therefore restricted to polypeptidic nanoparticles.[27,28] In contrast, the only two CKA-based degradable systems resulting from polymerization in aqueous dispersed media are obtained from conventional, free-radical polymerization in (mini)emulsion[29,30]

Very recently, thionolactones have been proposed as a new class of cyclic monomers suitable for rROP, whose insertion results in cleavable thioester units in the main chain (Figure 1a).[8] Their polymerization is based on thiocarbonyl addition–ring-opening (TARO)[31] mechanism, which relies on a radical addition onto C=S function followed by fragmentation via β-scission. In particular, copolymerization of dibenzo[c,e]oxepane-5-thione (DOT) with traditional vinyl monomers has recently been first reported by Roth[32-34] and Gutekunst,[31] and followed by others.[35-37] Interestingly, DOT exhibits several key benefits compared to CKAs, such as a high stability in protic solvents, an easy synthesis[32] and a quantitative ring opening during polymerization. The use of DOT also results in much higher reactivity ratios when copolymerized with acrylates. For instance with methyl acrylate (MA), r_{DOT} = 0.003 and r_{MA} = 0.424 whereas with 2-methylene-1,3-dioxepane (MDO), r_{MDO} = 0.00235 and r_{MA} = 26.535.[31,32] This was successfully illustrated to reversible addition-fragmentation chain transfer (RAFT) copolymerizations of DOT with acrylamides,[33] acrylonitrile,[33] acrylates[31,32] and even maleimide.[34] However, DOT inhibits the polymerization of vinyl acetate and *N*-vinylcarbazole, and acts as a bystander with methyl methacrylate.[32] Also, we recently reported the

conventional, free-radical emulsion copolymerization of DOT with vinyl monomers in presence of a surfactant.[38]

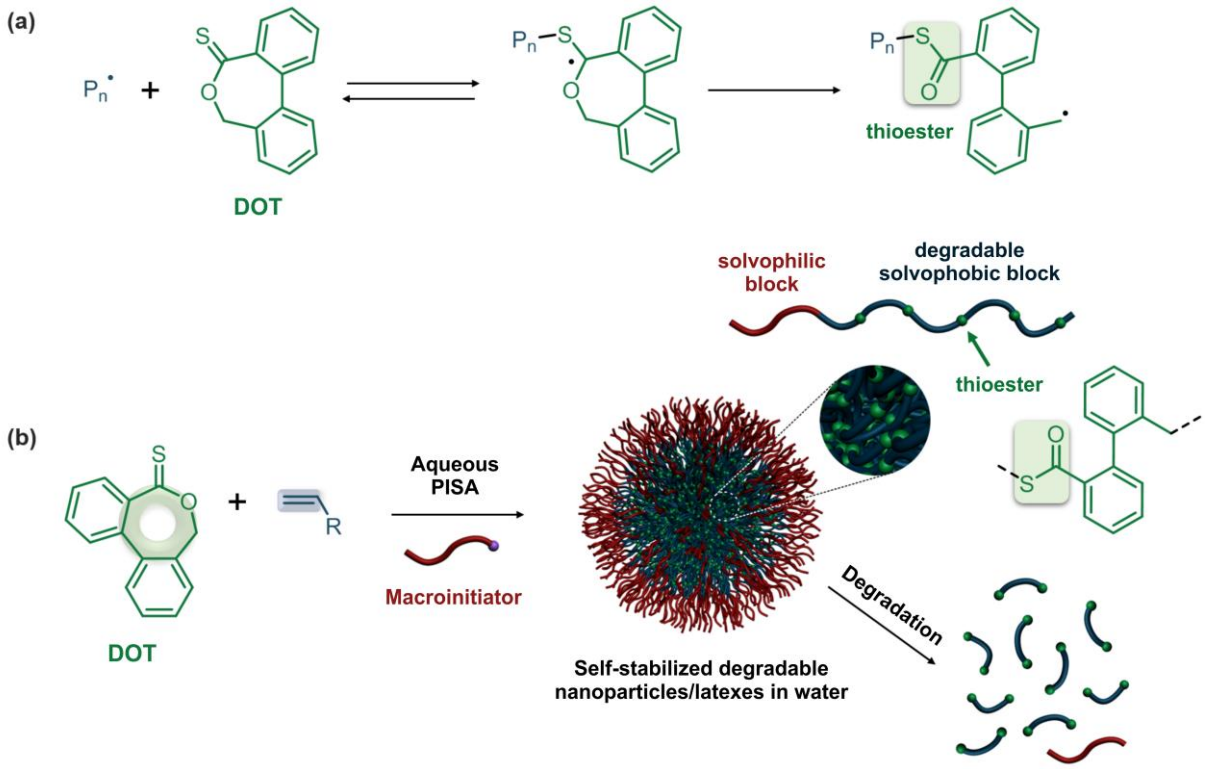

Figure 1. (a) Thiocarbonyl addition–ring-opening (TARO) copolymerization of dibenzo[c,e]oxepan-5-thione (DOT). (b) Synthesis of degradable vinyl polymer nanoparticles via aqueous nitroxide-mediated radical ring-opening copolymerization-induced self-assembly (rROPISA) of DOT and vinyl monomers from a water-soluble macroinitiator.

Herein, we report the first synthesis of degradable vinyl polymer latexes/nanoparticles by direct aqueous PISA (Figure 1b). This was achieved by building upon previous literature[39,40] and performing nitroxide-mediated polymerization (NMP) of DOT with either *n*BA or styrene (S), from a water-soluble macroalkoxyamine based on the nitroxide SG1. Spherical nanoparticles with long-term colloidal stability were obtained, which exhibited significant degradation under aminolytic and basic conditions. This study thus paves the way to the design of degradable waterborne PISA systems with different degradation modalities that could be of high interest for many areas such as biomedical applications (providing an

extension to biocompatible vinyl polymers), degradable coatings, sustained materials and plastics recycling; the latter of which has been recently addressed with DOT and its derivatives under homogeneous organic media by Johnson and co-workers.[36]

Experimental part

Materials

n-Butyl acrylate (*n*BA, ≥ 99 %), styrene (S, ≥ 99 %), potassium hydroxide (KOH, 90 %), potassium carbonate (K_2CO_3, ≥ 99 %), anhydrous dioxane (99.8 %) and isopropylamine (≥ 99 %) were purchased from Sigma-Aldrich and used as received. *N*-*tert*-butyl-*N*-(1-diethoxyphosphoryl-2,2-dimethylpropyl)aminoxy)-propionic acid alkoxyamine (BlocBuilder MA™, BB) and *N*-*tert*-butyl-*N*-[1-diethylphosphono-(2,2-dimethylpropyl)] nitroxide (SG1) were kindly supplied by Arkema. Acrylic acid (AA, > 99%) and 1,5,7-triazabicyclo[4.4.0]dec-5-ene (TBD, > 98%) were purchased from TCI. Deuterated chloroform ($CDCl_3$) and tetrahydrofuran (d_8-THF) were purchased from Eurisotop. Tetrahydrofuran (THF, HPLC grade) and chloroform ($CHCl_3$, HPLC grade) were obtained from VWR Chemicals. Hydrochloric acid (HCl, 37 %) was supplied by Carlo-Erba and trimethylsilyldiazomethane (2 M in hexane) was supplied from ACROS Organics. Dibenzo[c,e]oxepane-5-thione (DOT) was prepared as reported elsewhere using dibenzo[c,e]oxepin-5(7H)-one as intermediate (Figure S1).[32] Pressure glassware (tube 15 mL with plunger and round bottom flask 50 mL) were purchased from Sigma-Aldrich.

Analytical Methods

Nuclear magnetic resonance (NMR) spectroscopy

NMR spectroscopy was performed in 5 mm diameter tubes in D_2O, $CDCl_3$ or d_8-THF at 25 °C. ^1H NMR spectroscopy was performed on a Bruker Avance 3 HD 400 spectrometer operating at 400 MHz or on a Bruker Avance 300 spectrometer at 300 MHz for the determination of the conversion of AA. The chemical shift scale was calibrated based on the internal solvent signals: δ = 4.79 ppm for D_2O, δ = 7.26 ppm for $CDCl_3$ and δ = 3.58 ppm for d_8-THF.

Size exclusion chromatography (SEC)

SEC was performed at 35 °C with two columns from Polymer Laboratories (PL-gel MIXED-D; 300 × 7.5 mm; bead diameter, 5 µm; linear part, 400–400 000 g.mol^{-1}) and a differential refractive index detector (Spectrasystem RI-150 from Thermo Electron Corp.), using chloroform ($CHCl_3$) as eluent at a flow rate of 1 mL.min^{-1} and toluene as a flow-rate marker. A conventional calibration curve was based on poly(methyl methacrylate) (PMMA) standards (peak molar masses, M_p = 625–625 500 g.mol^{-1}) for PAA-*b*-P(*n*BA-*co*-DOT) copolymers and polystyrene (PS) standards (peak molar masses, M_p = 575–126 500 g.mol^{-1}) for PAA-*b*-P(S-*co*-DOT) copolymers from Polymer Laboratories. This technique allowed M_n (number-average molar mass), M_w (weight-average molar mass), and M_w/M_n (dispersity, $Đ$) to be determined. SEC of the degraded copolymers was performed in the presence of 0.1 % (v/v) of trifluoroacetic acid (TFA, 99 %) in chloroform (in both the mobile phase and the sample) to avoid the formation of aggregates and/or interaction with the columns and thiol chain ends.

Before SEC analysis, methylation of the carboxylic acid groups of the copolymers was performed using trimethylsilyldiazomethane.[41] 20 mg of dried copolymer was dissolved in THF (4 mL) and acidified by HCl_{aq}. (1 M) to reach a pH value of 1. Note that it was verified that the methylation conditions do not degrade model DOT-containing copolymers (Figure S2). A yellow solution of trimethylsilyldiazomethane (~0.5 mL) was then added dropwise at room temperature. Upon addition, bubbles formed and the solution became instantaneously colourless. Addition of the methylation agent was continued until the solution became yellow

and stopped bubbling. Then, an excess of methylation agent was added until the solution stays yellow, followed by stirring overnight at room temperature.

Dynamic light scattering (DLS)

Nanoparticle intensity-average diameter (D_z) and polydispersity index (PDI_{DLS}) were measured by dynamic light scattering (DLS) with a Nano ZS from Malvern (173° scattering angle) at a temperature of 25 °C. Nanoparticles were diluted in MilliQ water (dilution 1/10) prior to DLS measurements.

Transmission electron microscopy (TEM)

The morphology of PAA-*b*-P(S-*co*-DOT) nanoparticles was observed by TEM. Samples were diluted at 1.1 $mg.mL^{-1}$ in water prior analysis. 5 µL of diluted nanoparticle (NP) suspension was deposited on Formvar/carbon 400 Mesh Copper grid. After 5 min at room temperature, a drop of phosphotungstic acid 2 % filtered on 0.22 µm was added for negative staining during 30 s and the excess volume was removed with a blotting filter paper. The grids were then observed with a JEOL 1400 electron microscope operating at 80 kV. Digital images were directly recorded using a Gatan CCD camera.

The nanoparticles were analyzed by defining the number-average diameter ($D_{n,TEM}$), the weight-average diameter ($D_{w,TEM}$), the z-average diameter ($D_{z,TEM}$) and the polydispersity index (PDI_{TEM}) using equations described in Table S2.

Cryogenic transmission electron microscopy (cryo-TEM)

The morphology of PAA-*b*-P(*n*BA-*co*-DOT) nanoparticles was observed by cryo-TEM. For analysis, 5 µL of NP suspension diluted at 1.4 $mg.mL^{-1}$ prior analysis were deposited onto a Lacey Formvar/carbon 300 mesh copper grid (Ted Pella). The excess was manually blotted with a filter paper, and the residual thin film was immediately frozen by plunging into liquid ethane cooled down at liquid nitrogen temperature using a Leica EM-CPC cryoplunger. Observation was performed using a JEOL 2200FS field emission microscope (JEOL USA)

operating under an acceleration voltage of 200 kV in zero-loss mode (slit was 20 eV). High-magnification images (2k × 2k pixels) were recorded by a CCD camera (Gatan, Inc.) using Digital Micrograph software.

Synthetic procedures

*Synthesis of SG1-terminated poly(acrylic acid) macroinitiators (PAA-SG1) by NMP (**M1** and **M2**)*

In a typical synthesis (**M1**, Table S1), BB (1 eq., 0.5 mmol, 0.191 g), free SG1 (0.09 eq., 0.0045 mmol, 0.013 g), and AA (75 eq., 37.5 mmol, 2.703 g) were dissolved in dioxane (10 mL) and placed in a 15 mL Ace pressure tube with a magnetic bar. The tube was subjected to three freeze-pump-thaw degassing cycles, then back-filled with argon. The tube was placed in an oil bath at 115 °C for 1 h under nitrogen atmosphere stirred at 300 rpm. The conversion was determined by ^{1}H NMR in D_2O by integrating from 1.5 to 3.0 ppm, corresponding to the 3 vinylic protons of the polymer backbone (peaks *d* and *e*, Figure S3) and from 5.5 to 6.7 ppm (peaks *a–c*, Figure S3), corresponding to the 3 vinylic protons from the AA.[42] The resulting PAA-SG1 was then purified by precipitation in diethyl ether, filtered off, and then dried at room temperature under vacuum until constant weight to give a white and bright fine powder. The purified polymer was then analysed by SEC after methylation of the carboxylic acid groups. For the synthesis of **M2** (Table S1), the same procedure was performed with a polymerization time of 1.5 h.

*Synthesis of poly(acrylic acid)-b-poly(n-butyl acrylate-co-dibenzo[c,e]oxepane-5-thione) (PAA-b-P(nBA-co-DOT), (**A0-F1**) by aqueous emulsion rROPISA*

In a typical synthesis (**A1**, Table 1), *n*BA (400 eq., 16.4 mmol, 2.13 g) and DOT (4 eq., 0.168 mmol, 0.038 g, $f_{DOT,0}$ = 0.01, with $f_{DOT,0}$ the initial molar fraction of DOT) were added to an aqueous solution containing MilliQ water (12.5 mL), 3 mmol.L_{aq}^{-1} of NaOH (0.83 mmol, 0.033 g, 1 eq. of NaOH based on the total acrylic acid groups of PAA-SG1), K_2CO_3 (0.45 mmol, 0.062 g, 36 mmol.L_{aq}^{-1}) and the required amount of PAA-SG1 macroinitiator

(1 eq., 0.042 mmol, 0.075 g of **M1**). The solution was poured into a 50 mL-round-bottom pressure flask with a magnetic bar, bubbled with dry argon for 15 min at room temperature to remove dissolved oxygen and then immersed in a preheated oil bath at 120 °C (giving 110 °C in the reaction medium due to the internal pressure) for 3 h and stirred at 400 rpm. The solution was then rapidly cooled under air. The *n*BA conversion was determined by gravimetry. The dry extract was analysed by ^{1}H NMR in $CDCl_3$.The conversion of DOT was determined by ^{1}H NMR on the dry extract by integrating the 1H (Ar) of open DOT at 7.0 ppm and the 1H of DOT at 8.2 ppm. SEC measurements were performed after methylation of the carboxylic acid groups. The nanoparticle colloidal characteristics (D_z and PDI_{DLS}) were determined by DLS and their morphology was assessed by cryo-TEM.

The same procedure was repeated by independently varying the solids content (τ_s^{th}), $f_{DOT,0}$, the degree of polymerization of the PAA-SG1 macroinitiator ($DP_{n,PAA\text{-}SG1}$) and the solvophobic block ($DP_{n,P\mathit{n}BA}$), as follows: **A0** [*n*BA (400 eq., 16.4 mmol, 2.13 g) and **M1** (1 eq., 0.042 mmol, 0.075 g)]; **A2** [*n*BA (400 eq., 16.4 mmol, 2.13 g), DOT (8 eq., 0.347 mmol, 0.076 g, $f_{DOT,0}$ = 0.02) and **M1** (1 eq., 0.042 mmol, 0.075 g)]; **D1** [*n*BA (200 eq., 16.1 mmol, 2.068 g) and DOT (2 eq., 0.164 mmol, 0.037 g, $f_{DOT,0}$ = 0.01) and **M1** (1 eq., 0.08 mmol, 0.145 g)]; **E1** [*n*BA (600 eq., 16.8 mmol, 2.155 g) and DOT (6 eq., 0.170 mmol, 0.038 g, $f_{DOT,0}$ = 0.01) and **M1** (1 eq., 0.02 mmol, 0.050 g)] and **F1** [*n*BA (400 eq., 16.2 mmol, 2.076 g) and DOT (4 eq., 0.163 mmol, 0.037 g, $f_{DOT,0}$ = 0.01) and **M2** (1 eq., 0.041 mmol, 0.13 g)].

For kinetic monitoring, the same procedure was performed on the basis of **A1**. In five different 50 mL-round-bottom pressure flasks, the copolymerization of *n*BA and DOT was carried out for 30 min, 1.5 h, 2 h, 3 h and 5 h.

*Synthesis of poly(acrylic acid)-b-poly(styrene-co-dibenzo[c,e]oxepane-5-thione) (PAA-b-P(S-co-DOT), (**G0–2**) by aqueous emulsion rROPISA*

In a typical synthesis (**G2**, Table 1), S (400 eq., 12.7 mmol, 1.33 g) and DOT (8 eq., 0.261 mmol, 0.059 g, $f_{DOT,0}$ = 0.02) were added to an aqueous NaOH solution containing MilliQ

water (12.5 mL), 3 mmol.L_{aq}^{-1} of NaOH (0.64 mmol, 0.025 g, 1 eq. of NaOH based on the total acrylic acid groups of PAA-SG1), K_2CO_3 (0.45 mmol, 0.062 g, 36 mmol.L_{aq}^{-1}) and the required amount of PAA-SG1 macroinitiator (1 eq., 0.032 mmol, 0.058 g of **M1**). The solution was poured into a 50 mL-round-bottom pressure flask with a magnetic bar, bubbled with dry argon for 15 min at room temperature to remove dissolved oxygen and then immersed in a preheated oil bath at 120 °C (giving 110 °C in the reaction medium due to the internal pressure) for 6 h and stirred at 400 rpm. The solution was then rapidly cooled under air. The S conversion was determined by gravimetry. The dry extract was analysed by ^{1}H NMR in d_8-THF.The conversion of DOT was determined by ^{1}H NMR on the dry extract by integrating the 1H of PS closed to the open DOT units at 4.0 ppm and the 1H of DOT at 8.2 ppm. SEC measurements were performed after methylation of the carboxylic acid groups. The nanoparticle colloidal characteristics (D_z and PDI_{DLS}) were determined by DLS and their morphology was assessed by TEM.

The same procedure was repeated by varying $f_{DOT,0}$ as follows: **G0** [S (400 eq., 12.7 mmol, 1.33 g) and **M1** (1 eq., 0.032 mmol, 0.058 g)] and **G1** [S (400 eq., 12.7 mmol, 1.33 g), DOT (4 eq., 0.128 mmol, 0.029 g, $f_{DOT,0}$ = 0.01) and **M1** (1 eq., 0.032 mmol, 0.058 g)].

For kinetic monitoring, the same procedure was performed on the basis of **G1** with $f_{DOT,0}$ = 0.01. In six different 50 mL-round-bottom pressure flasks, the copolymerization of S and DOT was carried out for 1 h, 2 h, 3 h, 4 h, 5 h and 6 h.

Degradation procedures

Degradation of the copolymers by TBD

10 mg of dry extract was solubilized in 0.5 mL of THF for 2 h before adding 0.5 mL of solution at 5 wt.% of TBD in THF. The solution was stirred for 16 h at room temperature. The degradation reaction was quenched by adding HCl solution (1 M) until a pH of 1 is reached before performing methylation. The degradation products were analyzed by SEC.

Degradation of the copolymers by isopropylamine

10 mg of dry extract was solubilized in 1 mL of THF for a 2 h before adding 1 mL of isopropylamine. The solution was stirred for 16 h at room temperature. THF and isopropylamine were removed under vacuum before performing methylation. The degradation products were analyzed by SEC.

Degradation of the nanoparticles by TBD

In a typical procedure, 0.2 mL of nanoparticles (**A1**, τ_s^{th} = 15 wt.%) was added to 2.8 mL of MilliQ water containing 30 mg of TBD to reach a final concentration of 1 wt.% of nanoparticles and 1 wt.% of TBD. The solution was stirred for 48 h at room temperature. The degradation reaction was quenched by adding HCl solution (1 M) until pH 1 was reached before performing methylation. The degradation products were analyzed by SEC. Degradation of nanoparticles **A1** was also performed with a 5-fold higher concentration of TBD.

Degradation of the nanoparticles by isopropylamine

In a typical procedure, 0.2 mL of nanoparticles (**A1**, τ_s^{th} = 15 wt.%) was added to 2.8 mL of MilliQ before adding 3 mL of isopropylamine. The solution was stirred for 48 h at room temperature. Isopropylamine was removed under vacuum before performing methylation. The degradation products were analyzed by SEC.

Results and Discussion

A well-defined SG1-terminated poly(acrylic acid) macroalkoxyamine (PAA_{20}-SG1) was first synthesized as the solvophilic block by NMP of AA in dioxane using BB as alkoxyamine (**M1**, conv. AA = 21 mol.%, M_n = 1 800 g.mol^{-1}, $Đ$ = 1.1, DP_n = 20, Table S1). A low conversion

was targeted in order to promote high living chain fraction and therefore efficient reinitiation during chain extension. Aqueous emulsion PISA was then performed at 110 °C in presence of DOT and *n*BA (or S) (Figure 2).

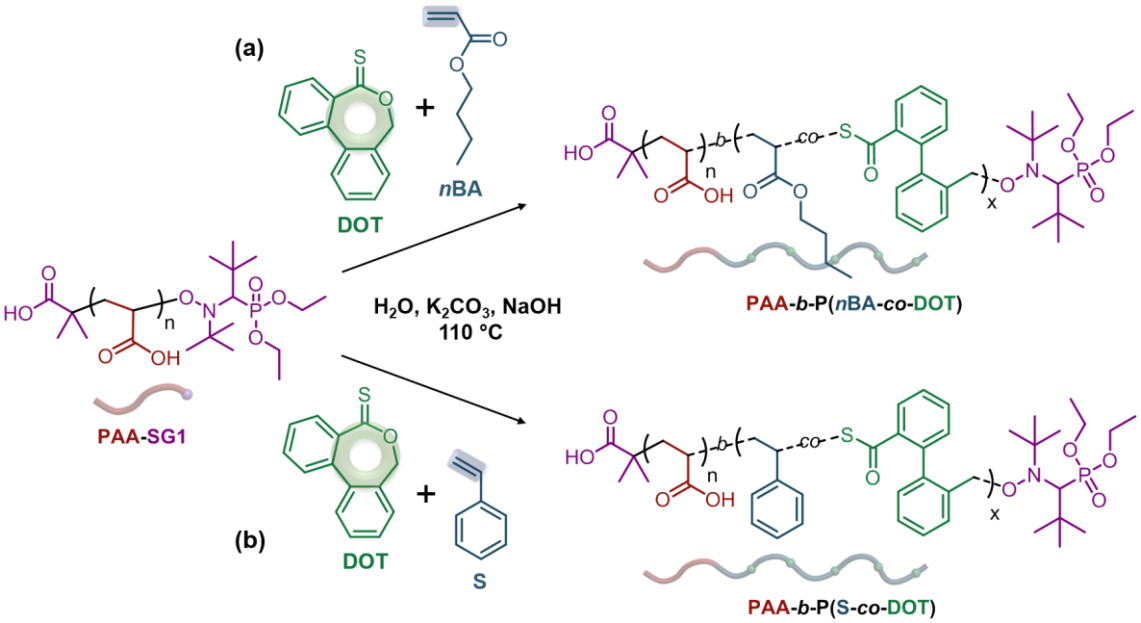

Figure 2. Synthesis of: (a) poly(acrylic acid)-*b*-poly(*n*-butyl acrylate-*co*-dibenzo[c,e]oxepane-5-thione) (PAA-*b*-P(*n*BA-*co*-DOT)) and (b) poly(acrylic acid)-*b*-poly(styrene-*co*-dibenzo[c,e]oxepane-5-thione) (PAA-*b*-P(S-*co*-DOT)) diblock copolymer nanoparticles by via aqueous nitroxide-mediated radical ring-opening copolymerization-induced self-assembly (rROPISA) of DOT and *n*-BA (or S) from a SG1-terminated poly(acrylic acid) macroalkoxyamine (PAA-SG1).

To ensure complete water-solubility of the macroinitiator during aqueous emulsion rROPISA, an aqueous solution of poly(sodium acrylate)$_{20}$-SG1 (PANa$_{20}$-SG1) was first prepared by reacting the PAA$_{20}$-SG1 macroalkoxyamine with 1 eq. NaOH (with respect to AA units), followed by addition of K_2CO_3 as a buffer to ensure stability of the SG1 nitroxide.[43] A mixture of DOT and *n*BA (or S) to achieve $f_{DOT,0}$ = 1 or 2 mol.% was added to the aqueous solution of macroinitiator to perform the rROPISA (higher $f_{DOT,0}$ values were not considered because of its low solubility in both comonomers[38]). Different parameters (solids content, $f_{DOT,0}$, $DP_{n,PAA\text{-}SG1}$ and $DP_{n,PnBA}$) were varied to explore the aqueous emulsion rROPISA process (Table 1).

Table 1. Experimental conditions and macromolecular characteristics for the synthesis of PAA-*b*-P(*n*BA-*co*-DOT) and PAA-*b*-P(S-*co*-DOT) diblock copolymer nanoparticles obtained by aqueous emulsion rROPISA at 110°C.

	Entry	$DP_{n,\,PAA\text{-}SG1}$	$f_{DOT,0}$[a] (mol.%)	t (h)	τ_s[th] (wt.%)	$DP_{n,th}$[b]	Conv. *n*BA/S[c] (wt.%)	$M_{n,th}$[d] (g.mol^{-1})	M_n[e] (g.mol^{-1})	$Đ$[e]	D_z[f] (nm)	PDI_{DLS}[f]	F_{DOT}[g] (mol.%)	f[h]
*n*BA	**A0**	20	0	3	15	400	72	38 700	79 900	2.4	95	0.14	0	0.47
	A1[h]	20	1.0	3	15	400	59	32 000	72 300	1.9	88	0.04	1.1	0.43
	A2	20	2.0	8	15	400	53	29 000	56 700	1.7	90	0.10	3.0	0.50
	B1	20	1.0	10	5	400	50	27 400	33 000	1.9	77	0.12	1.7	0.83
	C1	20	1.0	3	25	400	76	40 800	88 700	1.6	79	0.09	1.1	0.45
	D1	20	1.0	3	15	200	51	14 900	57 600	1.5	82	0.13	1.3	0.24
	E1	20	1.0	3	15	600	53	42 600	113 600	2.2	115	0.04	1.3	0.37
	F1	40[i]	1.0	3	15	400	63	35 500	81 500	1.7	81	0.07	1.2	0.42
S	**G0**	20	0	6	10	400	50	22 600	86 600	1.5	78	0.24	0	0.25
	G1	20	1.0	6	10	400	62	27 600	69 800	1.9	82	0.25	1.3	0.38
	G2	20	2.0	6	10	400	29	13 900	37 400	2.1	88	0.28	3.8	0.34

[a] Initial molar fraction of DOT in the reaction medium. [b] Theoretical DP_n for *n*BA or S. [c] Determined by gravimetry (conversions of DOT were found nearly quantitative by ^{1}H NMR). [d] Determined according to: $M_{n,th} = M_{n,PAA\text{-}SG1} + DP_{n,th}$ x conv. x $MW_{nBA\ or\ S}$ (contribution of DOT was neglected). [e] Determined by SEC in $CHCl_3$ on the methylated dry extract. [f] Determined by DLS. [g] Molar fraction of DOT in the copolymer, determined by ^{1}H NMR on the dry extract by integrating the 1H (Ar) of open DOT at 7.0 ppm and the 3H of (-CH3) of P*n*BA at 0.9 ppm, and by integration of 1H of S units close to open DOT units at 4 ppm and the 2H (-CH2) of PS at 1.5 ppm. [h] Determined according to: $f = (M_{n,th} - M_{n,PAA\text{-}SG1}) / (M_n - M_{n,PAA\text{-}SG1})$. [i] Note that the polymerization kinetics for **A1** in Figure 3 was continued to a higher conversion. [j] Obtained from PAA-SG1 **M2** (Table S1).

Copolymerization of DOT ($f_{DOT,0}$ = 0.01) with *n*BA at a solids content of 15 wt.% was first considered (**A1**, Figure 3, Table 1). After 3 h of polymerization, 59 wt.% conversion of *n*BA was obtained, which is slightly lower than the same experiment performed in absence of DOT (**A0**, Table 1), in agreement with the retardation effect of DOT.[32] Importantly for **A1**, the reaction medium changed from an orange heterogeneous suspension to a white homogeneous suspension upon polymerization, suggesting both formation of particles and

opening of DOT (as reported by Gutekunst and co-workers).[31] Almost complete conversion of DOT was reached after 3 h (96 %, Figure 3.a) and incorporation of thionolactone units into the P*n*BA backbone was confirmed by ^{1}H NMR spectroscopy of a dry extract. It showed a broader aromatic peak with a lower chemical shift at 7.0-8.0 ppm, characteristic of open DOT units[32] (Figure 3b). Integrating the aromatic protons of DOT at 7.0 ppm (peak *g*), and the methyl protons of P*n*BA at 0.9 ppm (peak *a*) gave an insertion of 1.1 mol.% of DOT (F_{DOT} = 0.011) in the copolymer after 3 h. SEC measurements performed on methylated dry extracts (to avoid interaction of acrylic acid units with the columns) gave M_n = 79.9 and 72.3 kg.mol^{-1} for **A0** and **A1**, respectively, as well as initiation efficiencies (*f*) of about 0.43–0.47 (Table 1). This is expected from nitroxide-mediated PISA due to a rather slow initiation process in the water-phase.[39,40] The controlled nature of the copolymerization for **A1** was demonstrated by the linear evolution of: (i) the logarithmic conversion before and after the nucleation, occurring after ~2 h of reaction (Figure S4) and (ii) the M_n with *n*BA conversion (Figure 3.c), despite increasing dispersity from ~1.5 to 2.4 above 80% conversion.**Figure 3.** This is commonly observed during the radical polymerization of *n*BA due to transfer to polymer and formation of dead chains at rather high monomer conversion.[44] Nonetheless, the dispersity was improved in presence of DOT as $Đ_{A0}$ = 2.4 vs. $Đ_{A1}$ = 1.9 after 3 h (Table 1 and Figure S5), highlighting its ability to reduce transfer reactions. Interestingly, F_{DOT} decreased from 4 to 0.9 mol.% during the copolymerization, which is explained by the faster consumption of DOT when copolymerized with acrylates (Figure 3.a),[31] thus leading to gradient-type copolymers.

The initial DOT content in the comonomer feed was then increased up to $f_{DOT,0}$ = 0.02 (**A2**, Table 1). Because of the retardation effect from DOT, it resulted in an even slower copolymerization kinetics, giving 53 wt.% conversion in *n*BA after 8 h with M_n = 29.6 kg.mol^{-1} and $Đ_{A2}$ = 1.7. As expected, it led to an increase in the DOT content to 3 mol.%.

The solids content was then varied from 5 to 25 wt.% for a constant $DP_{n,th}$ (see **B1** and **C1**, respectively, Table 1) to evaluate the working range of the aqueous emulsion rROPISA process. Increasing τ_s^{th} resulted in an increase in copolymerization rate as 50, 59

and 76 wt.% conversion in *n*Ba were obtained in 10 h for **B1**, and in 3h for **A1** and **C1**, respectively (Table 1). However, **C1** gave rise to formation of a fraction of coagulum on the side of the flask at the emulsion/air interface (representing ~15 wt.% of the initial monomer mass). While this may highlight the fact that there are not enough diblock copolymers to stabilize the newly created particles, it may also illustrate the limitations of our experimental setup, as the use of an industrial reactor with an optimized stirring/heating system could certainly have mitigated if not solved this problem. Increasing the length of the solvophilic block could also improve the colloidal properties at higher solids content.

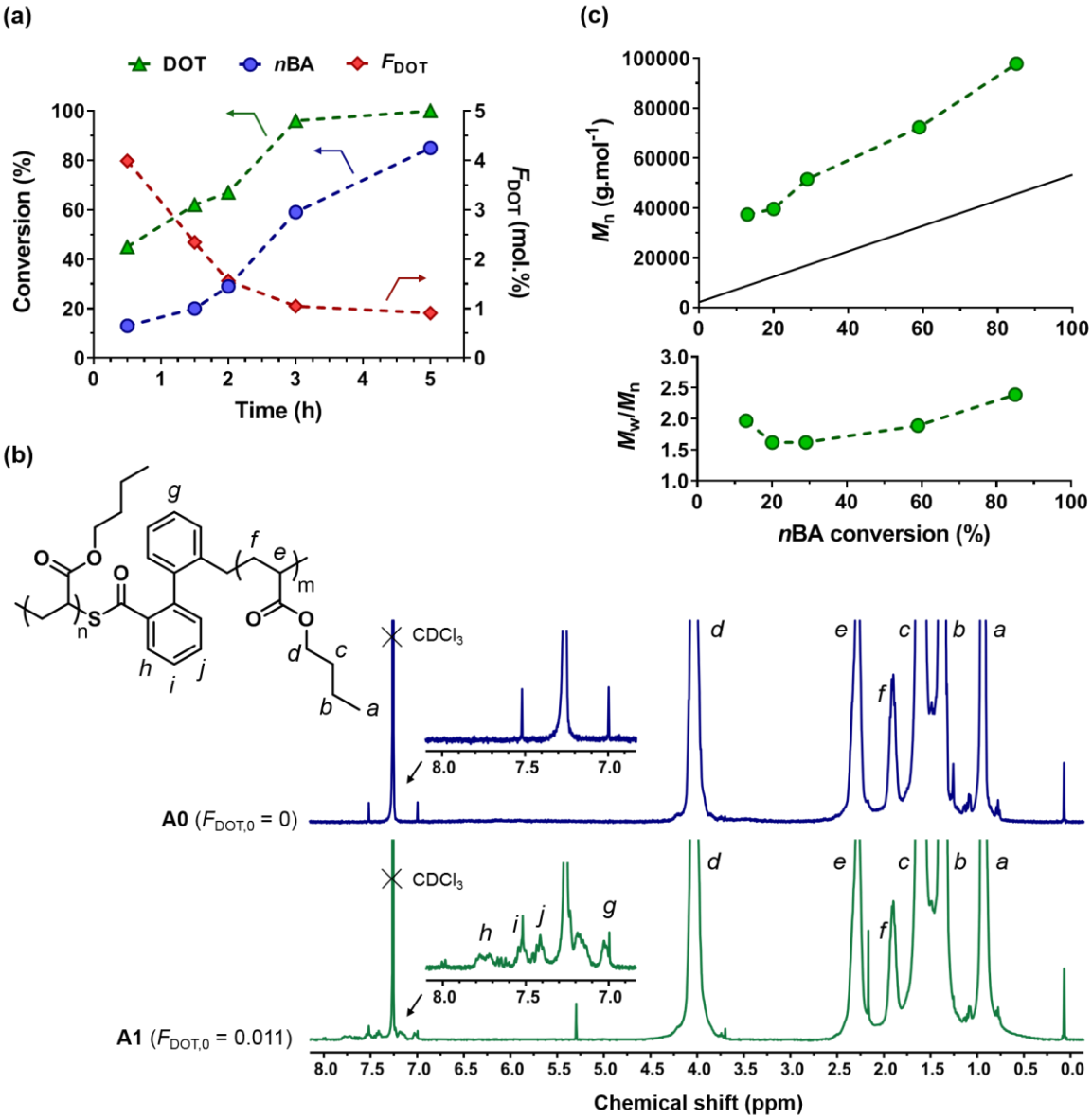

Figure 3. Synthesis of PAA-*b*-P(*n*BA-*co*-DOT) nanoparticles by copolymerization of *n*BA and DOT in water at 110 °C initiated by a $PANa_{20}$-SG1 macroalkoxyamine (**A1**, Table 1): (a) evolution of *n*BA conversion, DOT conversion and average molar fraction of DOT (F_{DOT}) in the copolymer vs. time; (b) ^{1}H NMR spectrum (400 MHz, $CDCl_3$) in the 0–8 ppm region of PAA-*b*-P(*n*BA-*co*-DOT) copolymers **A0** and **A1**; (c) evolution of M_n and $Đ$ vs. *n*BA conversion.

From the colloidal viewpoint, **A0** ($f_{DOT,0}$ = 0) and **A1** ($f_{DOT,0}$ = 0.01) experiments both yielded stable copolymer nanoparticles, exhibiting low average diameters (D_z = 88-95 nm) and narrow size distributions (PDI_{DLS} = 0.04-0.14) as measured by DLS (Table 1), hence showing minimal effect from the presence of DOT. $DP_{n,PnBA}$ and $DP_{n,PAA\text{-}SG1}$ were then varied to modulate the colloidal characteristics of the nanoparticles. When the targeted $DP_{n,PnBA}$ was

varied from 200 (**D1**, Table 1) to 600 (**E1**, Table 1), the average diameter progressively increased from 82 nm up to 115 nm, which originated from an increase in nanoparticle core size. On the other hand, using a longer macroalkoxyamine with $DP_{n,PAA\text{-}SG1}$ = 40 (**M2**, Table S1) led to similar nanoparticles compared to **A1** (**F1**, Table 1). The colloidal stability of all the nanoparticles was assessed over a period of one month during which average diameters remained constant with low particle size distributions (Figure 4 and S6). Moreover, PAA-*b*-P(*n*BA-*co*-DOT) nanoparticles **A1**, **A0**, **E1** and **F1** were visualized by cryo-TEM (Figure 4b and S7) which revealed spherical morphologies.

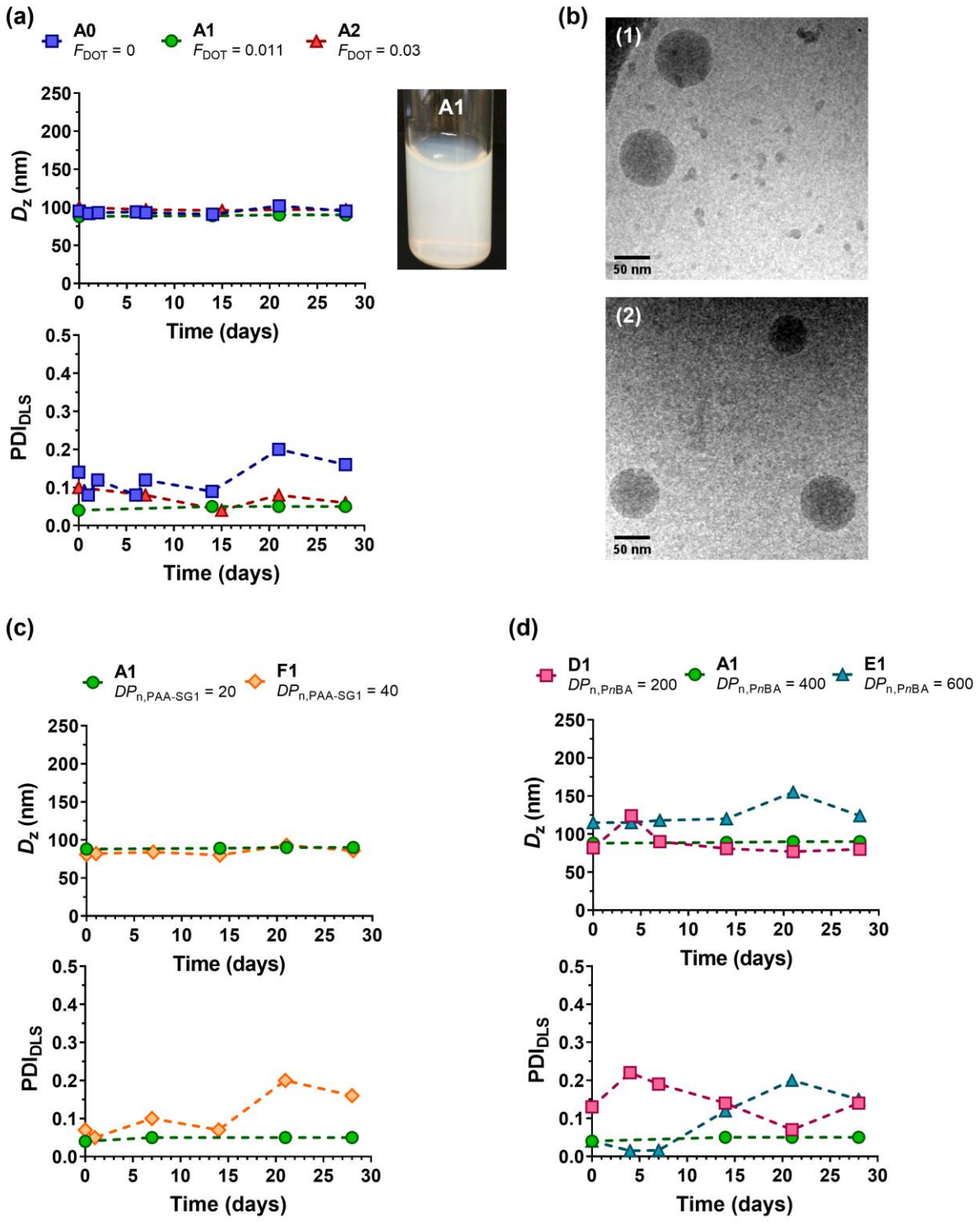

Figure 4. Colloidal properties of PAA-*b*-P(*n*BA-*co*-DOT) nanoparticles (**A0**, **A1**, **A2**, **D1**, **E1** and **F1,** Table 1). Variation of the intensity-average diameter (D_z) and polydispersity index (PDI_{DLS}) with time measured by DLS as function of: (a) F_{DOT}, (c) $DP_{n,PAA-SG1}$ and (d) $DP_{n,PnBA}$. (b) Representative cryo-TEM images of nanoparticles: (1) **A0** and (2) **A1** (Table 1). Note that the small objects in presence of nanoparticles are ice crystals.

Copolymerization of DOT ($f_{DOT,0}$ = 0.01) with S under the same experimental conditions than **A1** was then considered at a solids content of 10 wt.% (**G1**, Table 1). For higher τ_s^{th} values, colloidal instability characterized by polymer film formation at the water/air interface occurred. After 6 h, 62 wt.% conversion of S was reached (Figure 5a), which is comparable to the same experiment performed in absence of DOT (**G0**, Table 1). DOT was completely consumed after 3 h and insertion of thioester units was confirmed by ^{1}H NMR spectroscopy in d_8-THF on a dry extract, by integrating tertiary protons from S units close to open DOT units at 4 ppm (peak *b'*) and the methylenic protons of S (peak *a*) at 1.1-1.55 ppm (Figure 5b). Like **A1**, the faster incorporation of DOT during the copolymerization led to a decrease in F_{DOT} with S conversion from 5.3 to 1.3 mol.% (Figure 5a). While it has been shown that DOT does not easily copolymerize with S in anisole at 80°C,[31,32,37] its free-radical aqueous emulsion copolymerization at the same temperature showed a more homogeneous distribution of DOT units in the PS backbone, due to a compartmentalisation effect and/or the absence of solvent.[38] Our results also confirm the strong effect of increasing temperature which tends to drastically promote DOT incorporation, as recently shown during its free-radical copolymerization with S in anisole at 150 °C.[37] In addition, the expected difference in water solubility between DOT and S may also result in a higher concentration of DOT in the growing particles and thus a faster consumption. Linear evolution of M_n with S conversion up to M_n = 69.8 kg.mol^{-1} ($Đ_{G1}$ = 1.9) was obtained for **G1** (Figure 5c).The initiator efficiency was calculated to be f ~ 40 %, which is in line with the previous literature on emulsion PISA by NMP.[39] Compared to *n*BA (**A1**, $f_{DOT,0}$ = 0.1), faster incorporation of DOT was obtained, with 94 % DOT conversion after 2 h of reaction, as well as a lower conversion of S. Increasing the initial DOT content in the comonomer feed to $f_{DOT,0}$ = 0.02 (**G2**, Table 1 and Figure S8) led to a slowdown of the copolymerization kinetics, which reached 29 wt.% of conversion in S after 6 h (M_n = 37.4 kg.mol^{-1}, $Đ_{G2}$ = 2.1). As expected, this also successfully resulted in an increase in the DOT content in the copolymer to 3.8 mol.%.

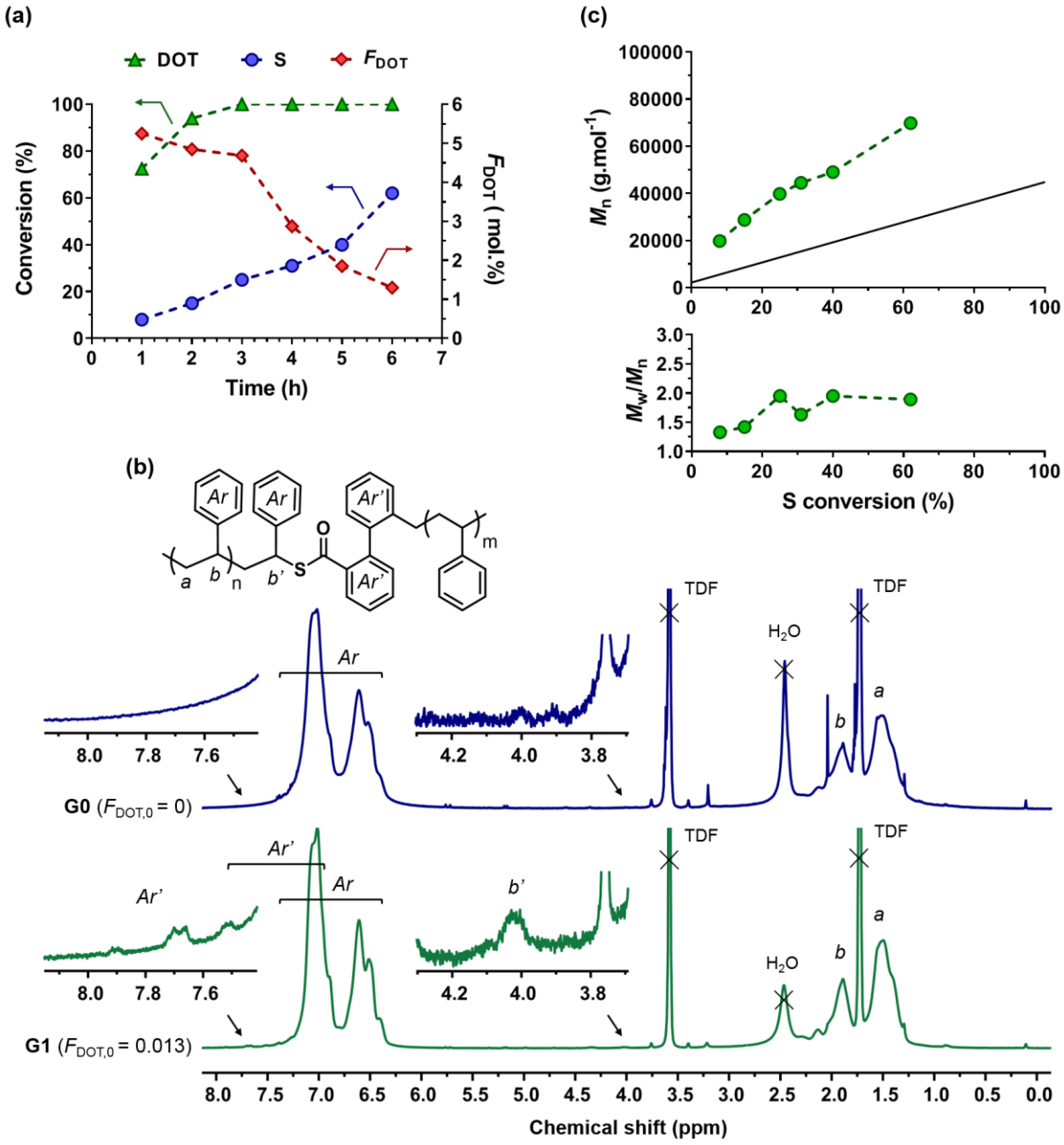

Figure 5. Synthesis of PAA-*b*-P(S-*co*-DOT) nanoparticles by copolymerization of S and DOT in water at 110 °C initiated by a $PANa_{20}$-SG1 macroalkoxyamine (**G1**, Table 1): (a) evolution of S conversion, DOT conversion and average molar fraction of DOT (F_{DOT}) in the copolymer vs. time; (b) ^{1}H NMR spectrum (400 MHz, d_8-THF) in the 0–8 ppm region of PAA-*b*-P(S-*co*-DOT) copolymers **G0** and **G1** and (c) evolution of M_n and $Đ$ vs. S conversion.

As for PAA-*b*-P(*n*BA-*co*-DOT) nanoparticles, DLS measurements also revealed the formation of stable dispersions of nanoparticles **G0–2** with a constant average diameter over at least

one month (D_z ~80-90 nm, Table 1, Figure 6a and S9), even though they exhibited a PDI_{DLS} > 0.2. Their spherical morphology was assessed by TEM, which also allowed to determine a number-average diameter $D_{n,TEM}$ of 32 nm and a PDI_{TEM} of 1.2-1.3 (Figure 6b and Table S2).

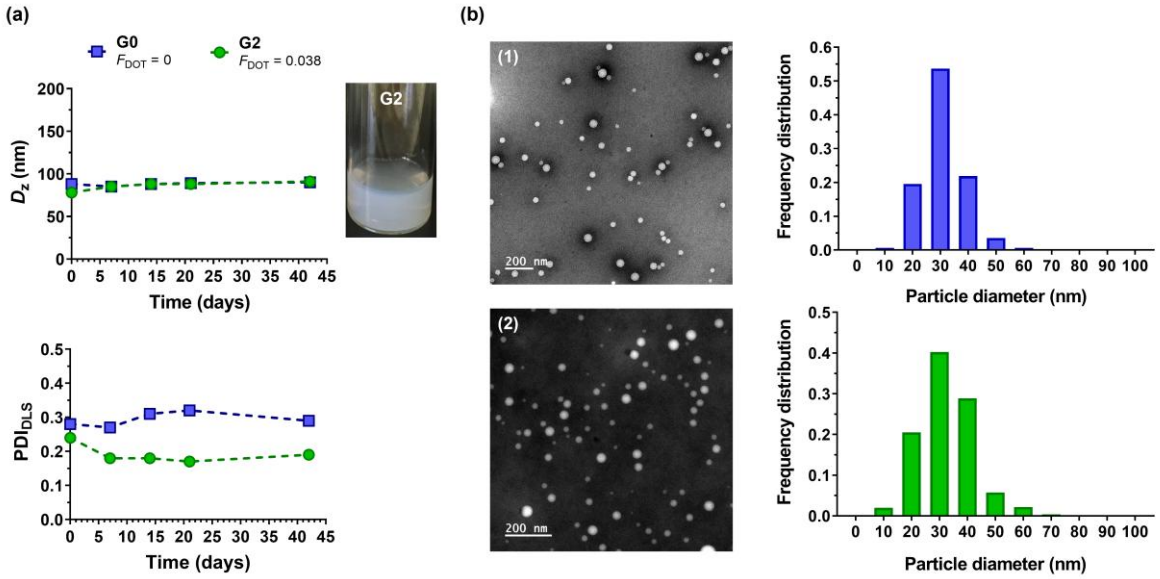

Figure 6. Colloidal properties of PAA-*b*-P(S-*co*-DOT) nanoparticles (**G0** and **G2**, Table 1). (a) Variation of the intensity-average diameter (D_z) and polydispersity index (PDI_{DLS}) with time measured by DLS. (b) Representative TEM images and associated size distribution (n = 500) for nanoparticles: (1) **G0** and (2) **G2**.

Degradation experiments on dry extracts were first performed to further confirmed the successful insertion of thioester groups into the copolymers and their susceptibility to cleavage under specific conditions. Thioester-containing copolymers can be cleaved by hydrolysis,[33] aminolysis,[31-33,38] methanolysis[31] and even thiolysis.[34] More recently, they have also been shown to degrade under physiological conditions in presence of cysteine or glutathione at concentrations mimicking extra- and intracellular conditions,[45] respectively. Herein, we used isopropylamine to perform aminolysis, as well as TBD as a strong base.[37]

As shown by SEC, all P(*n*BA-*co*-DOT) copolymer dry extracts exhibited significant decrease in M_n (77–93%) after degradation in presence of isopropylamine or TBD for 16 h

(Table 2, Figure 7 and S10). Conversely, the M_n of P*n*BA homopolymer **A0** ($f_{DOT,0}$ = 0) after degradation stayed constant (Table 2, Figure S11). Not only did these results confirm the successful incorporation of thioester units into P(*n*BA-*co*-DOT) copolymers, but they also suggested a weak gradient character as it did not prevent nearly complete degradations to occur. Interestingly, increasing F_{DOT} up to 0.03 (**A2**, Table 2) led to the highest M_n loss after degradation with either isopropylamine or TBD. Importantly, all these M_n values after degradation are in good agreement with the theoretical M_n of the degraded copolymers ($M_{n,deg.th}$, Table 2).

Direct degradation of the nanoparticles was also attempted. Although the degradation of P(*n*BA-*co*-DOT) nanoparticles in the presence of 1 wt.% TBD was less pronounced than the copolymers in solution, the M_n loss still reached 45–56 % at best after 48 h (see **A1**, **C1**–**F1**, Figure 7 and S10). The lower degradation for **A2** and **B1** nanoparticles can be explained by the much longer copolymerization times they required, which may promote branching reactions and formation of hydrophobic P*n*BA domains near the thioester functions, thus limiting the access of TBD. Also, the macromolecular PANa-based shell may also prevent efficient swelling of the nanoparticles by TBD. The degradation of nanoparticles **A1** was nonetheless significantly improved by either: (i) using a 5-fold higher concentration of TBD (-70% decrease in M_n, Figure 7a) or (ii) an isopropylamine/water (1/1, v/v) solution for 48 h (-79% decrease in M_n, Figure 7b), which showed similar degradation to that of copolymers in solution.

Table 2. Macromolecular characteristics of PAA-*b*-P(*n*BA-*co*-DOT) and PAA-*b*-P(S-*co*-DOT) nanoparticles obtained by aqueous emulsion rROPISA and their degradation products obtained under aminolytic or basic conditions.

							Dry extract		Nanoparticles
	Entry	$f_{DOT,0}$ (mol.%)	F_{DOT} [a] (mol.%)	M_n [b] (g.mol^{-1})	$Đ$ [b]	$M_{n,deg.th}$ [c] (g.mol^{-1})	$M_{n,deg.isop}$ [d] (g.mol^{-1}) (% M_n loss)	$M_{n,deg.TBD}$ [e] (g.mol^{-1}) (% M_n loss)	$M_{n,deg.TBD}$ [f] (g.mol^{-1}) (% M_n loss)
*n*BA	**A0**	0	0	79 900	2.4	-	79 500 (- 1 %)	78 700 (- 2 %)	77 100 (- 4 %)
	A1	1.0	1.1	72 300	1.9	11 800	12 500 (- 83 %)	9 900 (- 86 %)	40 000 (- 45 %)
	A2	2.0	3.0	56 700	1.7	4 400	4 600 (- 92 %)	4 000 (- 93 %)	47 500 (- 16 %)
	B1	1.0	1.7	33 000	1.9	7 600	7 500 (- 77 %)	5 200 (- 84 %)	30 800 (- 7 %)
	C1	1.0	1.1	88 700	1.6	11 800	14 800 (- 83 %)	12 500 (- 86 %)	42 800 (- 52 %)
	D1	1.0	1.3	57 600	1.5	10 000	10 300 (- 82 %)	9 000 (- 84 %)	29 800 (- 48 %)
	E1	1.0	1.3	113 600	2.2	10 000	10 000 (- 91 %)	9 700 (- 91 %)	50 000 (- 56 %)
	F1	1.0	1.2	81 500	1.7	10 800	15 500 (- 81 %)	9 700 (- 88 %)	42 000 (- 48 %)
S	**G0**	0	0	86 600	1.5	-	86 600 (- 0 %)	84 900 (- 2 %)	84 700 (- 2 %)
	G1	1.0	1.3	69 800	1.9	8 100	65 800 (- 6 %)	58 800 (- 16 %)	66 200 (- 5 %)
	G2	2.0	3.0	37 400	2.1	3 600	35 100 (- 5 %)	24 100 (- 35 %)	35 100 (- 5 %)

[a] Determined by ^{1}H NMR on the dry extract by integrating the 1H (Ar) of open DOT at 7.0 ppm and the 3H of (-CH_3) of P*n*BA at 0.9 ppm, and by integration of 1H of S close to open DOT units at 4 ppm and the 2H (-CH2-) of PS at 1.5 ppm. [b] Determined by SEC on dry extract. [c] Determined according to: $M_{n,deg.th} = [((1 - F_{DOT}) / F_{DOT}) \times MW_{nBA/S}] + MW_{DOT}$.[24] [d] Determined by SEC after degradation on dry extract dissolved at 5 mg.mL^{-1} in solution at 6.1 M of isopropylamine in THF, 25 °C, 16 h. [e] Determined by SEC after degradation on dry extract dissolved at 10 mg.mL^{-1} in solution at 2.5 wt.% of TBD in THF, 25 °C, 16 h. [f] Determined by SEC after degradation on nanoparticles dispersed at 1 wt.% in solution of H_2O containing 1 wt.% of TBD, 25 °C, 48 h.

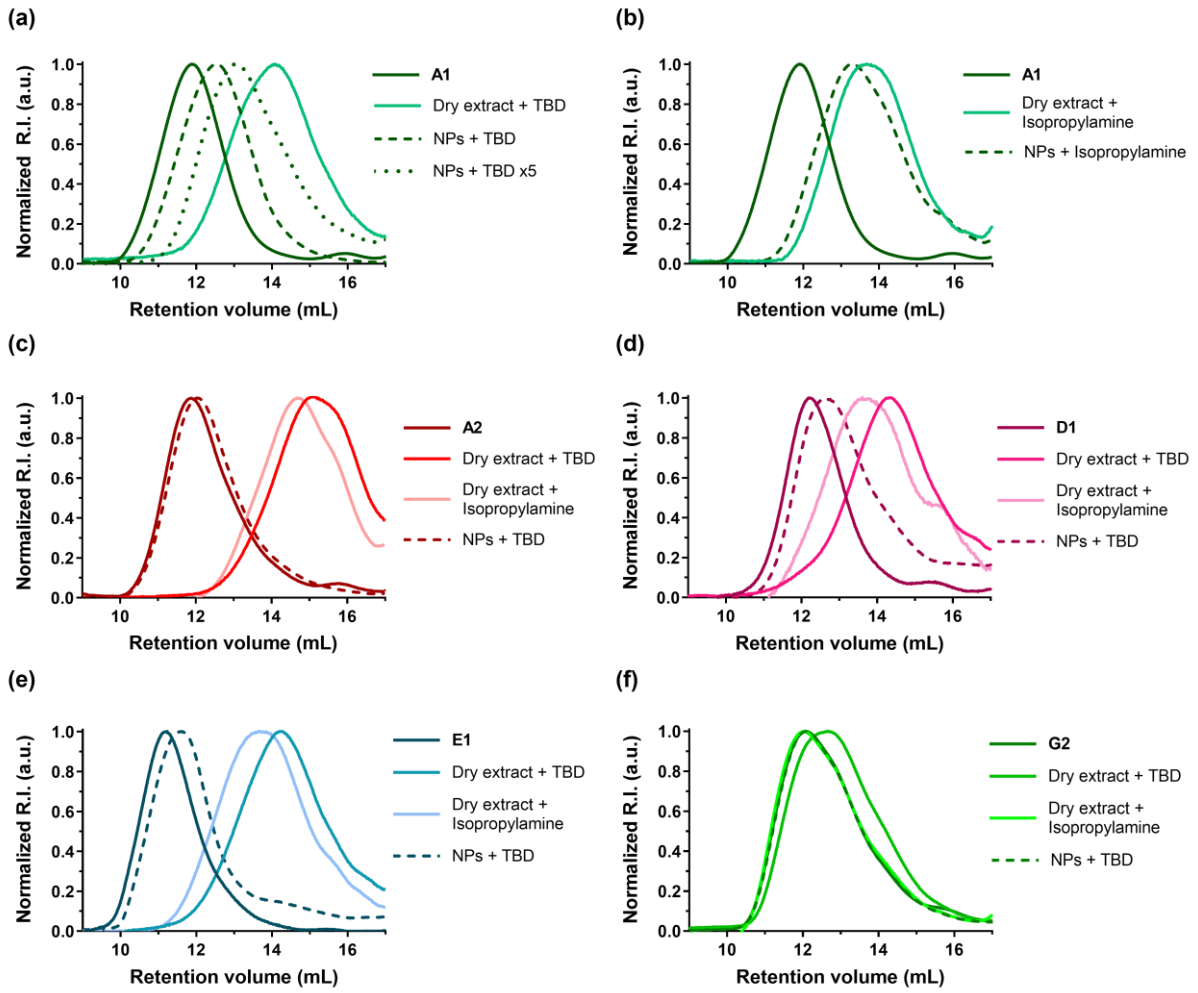

Figure 7. Evolution of SEC chromatograms of PAA-*b*-P(*n*BA-*co*-DOT) copolymers: (a) and (b) **A1**, (c) **A2**, (d) **D1**, (e) **E1** (Table 1) and PAA-*b*-P(S-*co*-DOT) copolymer (f) **G2** (Table 1), after degradation of dry extracts or nanoparticles (NPs) with isopropylamine or TBD.

Regarding P(S-*co*-DOT) copolymers **G1** and **G2**, only a significant degradation on the dry extracts with TBD was obtained, although it was lower than their *n*BA-based counterparts **A1** and **A2** (Figure 7f, S12-13 and Table 2). The decrease in M_n for **G1** and **G2** reached -16 % and -35 %, respectively, which is consistent with the increase in F_{DOT} between the two types of nanoparticles (F_{DOT} = 1.3 and 3.0, respectively). Conversely, no noticeable degradation (-5% decrease in M_n) was shown on both the dry extracts with isopropylamine and on the nanoparticles with TBD under the experimental conditions used. As DOT is consumed faster when copolymerized with S than with *n*BA (see Figure 3a and 5a), this results in a strong gradient character producing long PS sequences after cleavage of thioester groups. This

may explain the lower degradation for P(S-*co*-DOT) copolymers compared to that of P(*n*BA-*co*-DOT) copolymers **A1** and **A2**, despite similar F_{DOT} values. Moreover, absence of degradability of P(S-*co*-DOT) nanoparticles can also be explained by the restricted access of TBD to the core of the particles owing to the high T_g of PS (~100 °C).[38]

Conclusion

For the first time, the synthesis of degradable vinyl polymer nanoparticles/latexes by direct aqueous PISA is described. It relied on the rROPISA of DOT and *n*BA (or S) to insert labile thioester groups into the solvophobic block of vinyl copolymer nanoparticles. By adjusting the initial amount of DOT in the feed, the molar fraction of DOT in the resulting copolymers ranged from ~1 to ~3 mol.% for both vinyl monomers. Successful degradation under aminolytic or basic conditions on dry extracts (up to -93% decrease in M_n) and nanoparticles (up to -79% decrease in M_n) was demonstrated. The degradation of *n*BA-containing copolymers and nanoparticles was however more pronounced than that of their S-containing counterparts, probably due to a stronger gradient character and less accessibility of the nanoparticle core for the latter. Importantly, DOT insertion during the rROPISA process did not affect the colloidal properties of the nanoparticles as very stable suspensions were obtained exhibiting spherical morphologies with constant average diameters and relatively narrow particle size distributions at least one month. The study of higher order morphologies (throughout polymerization or during degradation) will be the subject of a future study. Given the extensive use of the PISA process, this work could open the door to a new generation of degradable nanoparticles/latexes for multiple applications ranging from nanomedicine to environmentally friendly materials and sustained/recyclable polymers.

Supporting Information

^{1}H NMR spectrum of DOT and PAA-SG1 macroinitiator **M1**, macromolecular characteristics of the PAA-SG1 macroinitiators **M1** and **M2**, kinetic data for the synthesis of **A1**, SEC traces of copolymers **A0**, **A1**, **G0**, **G2**, **B1**, **C1** and **F1** before (and after) degradation, DLS data of copolymer nanoparticles **A1**, **B1**, **C1,** and **G1**, TEM images of copolymer nanoparticles **E1** and **F1**, and TEM distributions of copolymer nanoparticles **G0** and **G2**. This information is available free of charge via the Internet at http://pubs.acs.org/.

Acknowledgments

The authors acknowledge the financial support from the Agence Nationale de la Recherche (grant number ANR-18-CE06-0014 CKAPART). We thank Dr. Sylvain Trepout (Institut Curie, Orsay, France) and PICT-Ibisa for the experiments using JEOL 2200FS TEM. This work has benefited from the facilities and expertise of the Platform for Transmission Electronic Microscopy of I2BC, Gif-sur-Yvette. The CNRS and University Paris-Saclay are also acknowledged for financial support. A previous version of this manuscript has been deposited on a preprint server (ChemRxiV, June 7, 2022; https://doi.org/10.26434/chemrxiv-2022-pf8k0)

References

1. Delplace, V.; Nicolas, J. Degradable vinyl polymers for biomedical applications. *Nature Chem.* **2015,** 7 (10), 771-784.
2. Tardy, A.; Nicolas, J.; Gigmes, D.; Lefay, C.; Guillaneuf, Y. Radical Ring-Opening Polymerization: Scope, Limitations, and Application to (Bio)Degradable Materials. *Chem. Rev.* **2017,** 117 (3), 1319-1406.
3. Agarwal, S. Chemistry, chances and limitations of the radical ring-opening polymerization of cyclic ketene acetals for the synthesis of degradable polyesters. *Polym. Chem.* **2010,** 1, 953-964.
4. Jackson, A. W. Reversible-deactivation radical polymerization of cyclic ketene acetals. *Polym. Chem.* **2020,** 11 (21), 3525-3545.
5. Bailey, W. J.; Ni, Z.; Wu, S. R. Free radical ring-opening polymerization of 4,7-dimethyl-2-methylene-1,3-dioxepane and 5,6-benzo-2-methylene-1,3-dioxepane. *Macromolecules* **1982,** 15 (3), 711-14.
6. Paulusse, J. M. J.; Amir, R. J.; Evans, R. A.; Hawker, C. J. Free Radical Polymers with Tunable and Selective Bio- and Chemical Degradability. *J. Am. Chem. Soc.* **2009,** 131 (28), 9805-9812.

7. Ratcliffe, L. P. D.; Couchon, C.; Armes, S. P.; Paulusse, J. M. J. Inducing an Order–Order Morphological Transition via Chemical Degradation of Amphiphilic Diblock Copolymer Nano-Objects. *Biomacromolecules* **2016,** 17 (6), 2277-2283.

8. Pesenti, T.; Nicolas, J. 100th Anniversary of Macromolecular Science Viewpoint: Degradable Polymers from Radical Ring-Opening Polymerization: Latest Advances, New Directions, and Ongoing Challenges. *ACS Macro Lett.* **2020,** 9 (12), 1812-1835.

9. D'Agosto, F.; Rieger, J.; Lansalot, M. RAFT-Mediated Polymerization-Induced Self-Assembly. *Angew. Chem., Int. Ed.* **2020,** 59 (22), 8368-8392.

10. Penfold, N. J. W.; Yeow, J.; Boyer, C.; Armes, S. P. Emerging Trends in Polymerization-Induced Self-Assembly. *ACS Macro Lett.* **2019,** 8 (8), 1029-1054.

11. Phan, H.; Taresco, V.; Penelle, J.; Couturaud, B. Polymerisation-induced self-assembly (PISA) as a straightforward formulation strategy for stimuli-responsive drug delivery systems and biomaterials: recent advances. *Biomater. Sci.* **2021,** 9 (1), 38-50.

12. Charleux, B.; Delaittre, G.; Rieger, J.; D'Agosto, F. Polymerization-Induced Self-Assembly: From Soluble Macromolecules to Block Copolymer Nano-Objects in One Step. *Macromolecules* **2012,** 45 (17), 6753-6765.

13. Warren, N. J.; Armes, S. P. Polymerization-Induced Self-Assembly of Block Copolymer Nano-objects via RAFT Aqueous Dispersion Polymerization. *J. Am. Chem. Soc.* **2014,** 136 (29), 10174-10185.

14. Canning, S. L.; Smith, G. N.; Armes, S. P. A Critical Appraisal of RAFT-Mediated Polymerization-Induced Self-Assembly. *Macromolecules* **2016,** 49 (6), 1985-2001.

15. Chen, S.; Cardozo, A. F.; Julcour, C.; Blanco, J.-F.; Barthe, L.; Gayet, F.; Lansalot, M.; D'Agosto, F.; Delmas, H.; Manoury, E.; Poli, R. Amphiphilic core-cross-linked micelles functionalized with bis(4-methoxyphenyl)phenylphosphine as catalytic nanoreactors for biphasic hydroformylation. *Polymer* **2015,** 72, 327-335.

16. Zhu, C.; Nicolas, J. (Bio)degradable and Biocompatible Nano-Objects from Polymerization-Induced and Crystallization-Driven Self-Assembly. *Biomacromolecules* **2022,** 23 (8), 3043-3080.

17. Wan, J.; Fan, B.; Thang, S. H. RAFT-mediated polymerization-induced self-assembly (RAFT-PISA): current status and future directions. *Chem. Sci.* **2022,** 13 (15), 4192-4224.

18. Yeow, J.; Boyer, C. Photoinitiated Polymerization-Induced Self-Assembly (Photo-PISA): New Insights and Opportunities. *Adv. Sci.* **2017,** 4 (7), 1700137.

19. Tan, J.; Sun, H.; Yu, M.; Sumerlin, B. S.; Zhang, L. Photo-PISA: Shedding Light on Polymerization-Induced Self-Assembly. *ACS Macro Lett.* **2015,** 4 (11), 1249-1253.

20. Parkatzidis, K.; Truong, N. P.; Rolland, M.; Lutz-Bueno, V.; Pilkington, E. H.; Mezzenga, R.; Anastasaki, A. Transformer-Induced Metamorphosis of Polymeric Nanoparticle Shape at Room Temperature. *Angew. Chem., Int. Ed.* **2022,** 61 (8), e202113424.

21. Mellot, G.; Guigner, J.-M.; Bouteiller, L.; Stoffelbach, F.; Rieger, J. Templated PISA: Driving Polymerization-Induced Self-Assembly towards Fibre Morphology. *Angew. Chem., Int. Ed.* **2019,** 58 (10), 3173-3177.

22. Foster, J. C.; Grocott, M. C.; Arkinstall, L. A.; Varlas, S.; Redding, M. J.; Grayson, S. M.; O'Reilly, R. K. It is Better with Salt: Aqueous Ring-Opening Metathesis Polymerization at Neutral pH. *J. Am. Chem. Soc.* **2020,** 142 (32), 13878-13885.

23. Varlas, S.; Foster, J. C.; O'Reilly, R. K. Ring-opening metathesis polymerization-induced self-assembly (ROMPISA). *Chem. Commun.* **2019,** 55 (62), 9066-9071.

24. Guégain, E.; Zhu, C.; Giovanardi, E.; Nicolas, J. Radical Ring-Opening Copolymerization-Induced Self-Assembly (rROPISA). *Macromolecules* **2019,** 52 (10), 3612-3624.

25. Zhu, C.; Denis, S.; Nicolas, J. A Simple Route to Aqueous Suspensions of Degradable Copolymer Nanoparticles Based on Radical Ring-Opening Polymerization-Induced Self-Assembly (rROPISA). *Chem. Mater.* **2022,** 34 (4), 1875-1888.

26. Zhu, C.; Nicolas, J. Towards nanoparticles with site-specific degradability by ring-opening copolymerization induced self-assembly in organic medium. *Polym. Chem.* **2021,** 12 (4), 594-607.

27. Grazon, C.; Salas-Ambrosio, P.; Ibarboure, E.; Buol, A.; Garanger, E.; Grinstaff, M. W.; Lecommandoux, S.; Bonduelle, C. Aqueous Ring-Opening Polymerization-Induced Self-Assembly (ROPISA) of N-Carboxyanhydrides. *Angew. Chem., Int. Ed.* **2020,** 59 (2), 622-626.

28. Grazon, C.; Salas-Ambrosio, P.; Antoine, S.; Ibarboure, E.; Sandre, O.; Clulow, A. J.; Boyd, B. J.; Grinstaff, M. W.; Lecommandoux, S.; Bonduelle, C. Aqueous ROPISA of α-amino acid N-carboxyanhydrides: polypeptide block secondary structure controls nanoparticle shape anisotropy. *Polym. Chem.* **2021,** 12 (43), 6242-6251.

29. Siebert, J. M.; Baumann, D.; Zeller, A.; Mailänder, V.; Landfester, K. Synthesis of Polyester Nanoparticles in Miniemulsion Obtained by Radical Ring-Opening of BMDO and Their Potential as Biodegradable Drug Carriers. *Macromol. Biosci.* **2012,** 12 (2), 165-175.

30. Carter, M. C. D.; Hejl, A.; Woodfin, S.; Einsla, B.; Janco, M.; DeFelippis, J.; Cooper, R. J.; Even, R. C. Backbone-Degradable Vinyl Acetate Latex: Coatings for Single-Use Paper Products. *ACS Macro Lett.* **2021,** 10 (5), 591-597.

31. Smith, R. A.; Fu, G.; McAteer, O.; Xu, M.; Gutekunst, W. R. Radical Approach to Thioester-Containing Polymers. *J. Am. Chem. Soc.* **2019,** 141 (4), 1446-1451.

32. Bingham, N. M.; Roth, P. J. Degradable vinyl copolymers through thiocarbonyl addition–ring-opening (TARO) polymerization. *Chem. Commun.* **2019,** 55 (1), 55-58.

33. Bingham, N. M.; Nisa, Q. u.; Chua, S. H. L.; Fontugne, L.; Spick, M. P.; Roth, P. J. Thioester-Functional Polyacrylamides: Rapid Selective Backbone Degradation Triggers Solubility Switch Based on Aqueous Lower Critical Solution Temperature/Upper Critical Solution Temperature. *ACS Appl. Polym. Mater.* **2020,** 2 (8), 3440-3449.

34. Spick, M. P.; Bingham, N. M.; Li, Y.; de Jesus, J.; Costa, C.; Bailey, M. J.; Roth, P. J. Fully Degradable Thioester-Functional Homo- and Alternating Copolymers Prepared through Thiocarbonyl Addition–Ring-Opening RAFT Radical Polymerization. *Macromolecules* **2020,** 53 (2), 539-547.

35. Gil, N.; Thomas, C.; Mhanna, R.; Mauriello, J.; Maury, R.; Leuschel, B.; Malval, J.-P.; Clément, J.-L.; Gigmes, D.; Lefay, C.; Soppera, O.; Guillaneuf, Y. Thionolactone as a Resin Additive to Prepare (Bio)degradable 3D Objects via VAT Photopolymerization**. *Angew. Chem., Int. Ed.* **2022,** 61 (18), e202117700.

36. Kiel, G. R.; Lundberg, D. J.; Prince, E.; Husted, K. E. L.; Johnson, A. M.; Lensch, V.; Li, S.; Shieh, P.; Johnson, J. A. Cleavable Comonomers for Chemically Recyclable Polystyrene: A General Approach to Vinyl Polymer Circularity. *J. Am. Chem. Soc.* **2022,** 144 (28), 12979-12988.

37. Gil, N.; Caron, B.; Siri, D.; Roche, J.; Hadiouch, S.; Khedaioui, D.; Ranque, S.; Cassagne, C.; Montarnal, D.; Gigmes, D.; Lefay, C.; Guillaneuf, Y. Degradable Polystyrene via the Cleavable Comonomer Approach. *Macromolecules* **2022,** 55 (15), 6680-6694.

38. Galanopoulo, P.; Gil, N.; Gigmes, D.; Lefay, C.; Guillaneuf, Y.; Lages, M.; Nicolas, J.; Lansalot, M.; D'Agosto, F. One-Step Synthesis of Degradable Vinylic Polymer-Based Latexes via Aqueous Radical Emulsion Polymerization. *Angew. Chem., Int. Ed.* **2022,** 61 (15), e202117498.

39. Delaittre, G.; Nicolas, J.; Lefay, C.; Save, M.; Charleux, B. Surfactant-free synthesis of amphiphilic diblock copolymer nanoparticles via nitroxide-mediated emulsion polymerization. *Chem. Commun.* **2005,** (5), 614-616.

40. Delaittre, G.; Nicolas, J.; Lefay, C.; Save, M.; Charleux, B. Aqueous suspension of amphiphilic diblock copolymer nanoparticles prepared in situ from a water-soluble poly(sodium acrylate) alkoxyamine macroinitiator. *Soft Matter* **2006,** 2 (3), 223-231.

41. Couvreur, L.; Lefay, C.; Belleney, J.; Charleux, B.; Guerret, O.; Magnet, S. First Nitroxide-Mediated Controlled Free-Radical Polymerization of Acrylic Acid. *Macromolecules* **2003,** 36 (22), 8260-8267.

42. Lefay, C.; Belleney, J.; Charleux, B.; Guerret, O.; Magnet, S. End-Group Characterization of Poly(acrylic acid) Prepared by Nitroxide-Mediated Controlled Free-Radical Polymerization. *Macromol. Rapid Commun.* **2004,** 25 (13), 1215-1220.

43. Charleux, B.; Nicolas, J. Water-soluble SG1-based alkoxyamines: A breakthrough in controlled/living free-radical polymerization in aqueous dispersed media. *Polymer* **2007,** 48 (20), 5813-5833.

44. Farcet, C.; Belleney, J.; Charleux, B.; Pirri, R. Structural Characterization of Nitroxide-Terminated Poly(n-butyl acrylate) Prepared in Bulk and Miniemulsion Polymerizations. *Macromolecules* **2002,** 35 (13), 4912-4918.

45. Bingham, N. M.; Nisa, Q. u.; Gupta, P.; Young, N. P.; Velliou, E.; Roth, P. J. Biocompatibility and Physiological Thiolytic Degradability of Radically Made Thioester-Functional Copolymers: Opportunities for Drug Release. *Biomacromolecules* **2022,** 23 (5), 2031-2039.